Gas Turbines Power Regulation Subject to Actuator Constraints, Disturbances and Measurement Noises

Nasiri, Ali; Bayat, Farhad; Mobayen, Saleh; Hossein Nia Kani, S.H.

DOI
10.1109/ACCESS.2021.3064893

Publication date
2021

Document Version
Final published version

Published in
IEEE Access

Citation (APA)
Nasiri, A., Bayat, F., Mobayen, S., & Hossein Nia Kani, S. H. (2021). Gas Turbines Power Regulation Subject to Actuator Constraints, Disturbances and Measurement Noises. *IEEE Access*, *9*, 40155-40164. https://doi.org/10.1109/ACCESS.2021.3064893

Received February 8, 2021, accepted March 4, 2021, date of publication March 9, 2021, date of current version March 17, 2021.
Digital Object Identifier 10.1109/ACCESS.2021.3064893

Gas Turbines Power Regulation Subject to Actuator Constraints, Disturbances and Measurement Noises

ALI NASIRI[1], FARHAD BAYAT[1], (Member, IEEE), SALEH MOBAYEN[1,2], AND S. HASSAN HOSSEINNIA[3], (Senior Member, IEEE)
[1]Department of Electrical Engineering, University of Zanjan, Zanjan 45371-38791, Iran
[2]Future Technology Research Center, National Yunlin University of Science and Technology, Yunlin 64002, Taiwan
[3]Department of Precision and Microsystems Engineering, Delft University of Technology, 2628 Delft, The Netherlands
Corresponding authors: Farhad Bayat (bayat.farhad@znu.ac.ir) and Saleh Mobayen (mobayens@yuntech.edu.tw)

ABSTRACT An accurate understanding of the output power functionality in gas turbines concerning the fuel, inlet valve status and other parameters can provide a general overview of the turbine's performance. In this study, the problem of practical power regulation in gas turbines is investigated in the simultaneous presence of actuator constraints, unknown disturbances, and measurement noises. To this aim, a model predictive controller-based approach is utilized because of its high flexibility combined with a two-layer filtering and anti-filtering procedure to efficiently cope with the measurement noises. Moreover, the proposed structure takes the effects of unknown disturbances into account and thereby it is shown that the proposed controller can efficiently achieve all design objectives while handling actuator constraints, disturbances and measurement noises.

INDEX TERMS Performance improvement, gas turbine, actuators constraints, model predictive control, estimation.

I. INTRODUCTION

The gas turbine is a rotating machine that works on the energy of combustion gases [1], [2]. Gas turbines are the significant and extensively employed prime movers in transportation industry [3]. The public perception is that the aircraft engine is one of the most widely used types of gas turbines [4], [5]. Besides this important application area, gas turbines are used in power systems where they are the main power generators [6]. Each gas turbine unit consists of a compressor for compressing air, a combustion chamber for mixing air with fuel and combustion, and a turbine for converting hot and compressed gas energy into mechanical energy [7]–[9]. Due to the increasing importance of gas turbines in various industries and the necessity of designing the proper control system for gas turbines as the beating heart of this industry, extensive research has been done in the recent years [10]–[13].

Obtaining a suitable model for a gas turbine and determining its various parameters can play a significant role in the stability of the power system [14]–[16]. The control system is the most important section of a gas turbine power plant [17]. Without a suitable control scheme, any variation in power demand or frequency deviation can lead to over-heating or over-speeding, or even system shutdown. In recent researches, several models for gas turbines have been of interest to experts, including IEEE, Rouen, thermodynamic and neural models, among which Rouen is more prominent. In [18], an accurate nonlinear three-order model is employed for investigation of the dynamic behavior of DEUTZ T216 gas turbine (which is used in the jet engine) and a controller is designed for the stabilization of the system using feedback linearization technique. Reference [19] provides good modeling of a low-power gas-turbine which is suitable for simulation. Once the model is extracted, the system constraints are mentioned which are necessary to better understanding of the system design and control. After extracting the model and identifying the constraints, an efficient controller is required and, as mentioned in [20], the Model Predictive Control (MPC) method, due to its high flexibility and dynamic constraints such as constraints on the state and nonlinear control variables, is an appropriate controller. The model predictive control scheme is considered as the control algorithm in this study. Reference [21] introduces an optimized and systematic way to find a linear feedback control law for a linearized version of a low-power gas turbine. In [22], a multivariate model of a gas turbine derived from the linearized system equations is investigated.

The associate editor coordinating the review of this manuscript and approving it for publication was Zhouyang Ren.

The model predictive control approach is an advanced high-performance design technique which is known to be a very efficient method of controlling complex [23]–[25], and non-minimum-phase systems [26], [27]. The simplicity, conceptual easiness and accurate tracking performance of MPC approach have led to widespread successful applications, such as energy and power systems [28]–[30], aero-space [31], [32], and automotive control [33], [34]. Furthermore, MPC is acknowledged for its ability of coping with constraints on the state, output and input variables. These features make the predictive control a distinct and superior method compared to other existing advanced controllers. In the MPC algorithm, at each sampling time, an open-loop sequence of settings of decision variables is calculated in order to optimize future behavior of the system, which eventually yields a sequence of appropriate input variables in the defined horizon for the control to apply to the system [35].

In [17], an adaptive MPC method with online parameter estimation is presented for a gas turbine, where the adaptive MPC is designed to maintain the speed and temperature responses of the gas turbine within their desired levels in the existence of frequency drop or changes in load demand. In [38], a fuzzy modeling approach and a fast MPC algorithm are employed for a gas turbine system to achieve the high-tracking performance, less settling time and disturbance rejection capability. A multi-objective MPC approach is proposed in [12] for the control of a gas turbine system, where the objective function of the MPC technique is formulated simultaneously considering economic indices, terminal cost function, and stability constraints. A multivariable nonlinear MPC technique is suggested in [39] to avoid the unsafe or unsuitable operation of gas turbines, while decreasing the NO_x emissions. In [40], the design approach of an online fully nonlinear MPC is proposed for a gas turbine system, where the reduced-order internal model used in the control approach is developed from an original high-order physics-based model.

To the best of authors' knowledge, the problem of gas turbine power regulation in the simultaneous presence of actuator constraints, external disturbances and measurement noise has not been completely addressed in the literature including the above-mentioned approaches. It is emphasized that there are some related research works that address only parts of these objectives. For example, in the most recent related work [17], constraints satisfaction and constant disturbance rejection objectives are considered. However, it does not propose any systematic way within the controller design procedure to reduce the effects of measurement noise on the closed-loop performance. On the contrary, in the current work, an efficient MPC-based controller is designed for gas turbine power regulation where a systematic procedure is proposed to simultaneously cope with actuator constraints, disturbances and measurement noises. In the first part, we deal with the modelling of the gas turbine and its principles of operation; then, we obtain a nonlinear dynamic model. In the second part, by linearization of this model, the predictive controller is designed for this linear model in the presence of actuators constraints, external disturbances and measurement noises. It is emphasized that in the proposed method a two-layer filtering and anti-filtering mechanism is incorporated within the MPC design procedure that has two features. First, the filter part leads to a significant reduction in the effects of measurement noise on the system performance. Second, the anti-filter part will recover the performance degradation of the nominal operation (without noise) because of using a filtering procedure.

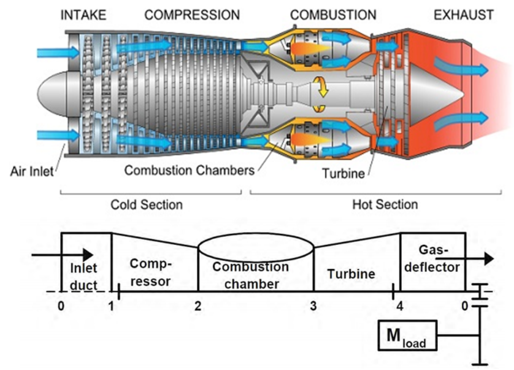

FIGURE 1. Main parts of a gas turbine.

The remaining content of this article is arranged as follows: in Section 2, the gas turbine model, containing the system description and the control-oriented gas turbine model is introduced. Then, the model predictive control technique for the gas turbine is proposed in Section 3. Besides, the CARIMA model for gas turbine is constructed and the gas turbine output prediction model with external disturbance and measurement noise is presented. In Section 4, the calculation of control law is presented. Furthermore, the performance of the control method is verified by simulation results in Section 5. Finally, conclusions are drawn in Section 6.

II. GAS TURBINE MODEL

A. GAS TURBINE MODEL

As illustrated in Fig. 1, the main parts of a gas turbine consist of the inlet, compressor, combustion chamber, turbine and nozzle or deflector. The turbine works based on the following cycles. First, air is drawn into the system and compressed in the compressor, then enters into the combustion chamber where fuel is continuously added to the air and the mixture is ignited. The resulting hot gases are expanded and passed first through the compressor turbine to keep it rotating, so that the engine is self-sustaining, and then the gas is exhausted through the power turbine via a variable orifice nozzle. When this cycle is repeated, it is vital to regulate the output variables, i.e. the gas generator speed and the temperature of the gas stream entering the power turbine, which affects the load speed. In addition, to prevent damage to the internal components of the turbine, for example the blades, the gas flow temperature must be limited. This critical issue makes the controller design procedure challenging.

B. CONTROL ORIENTED GAS TURBINE MODEL

Various control variables can be used to regulate the gas turbine output power; however, the fuel inlet to the combustion chamber, and the pressure valve angle of the turbine inlet are counted as a suitable choice due to their significant effect on all engine performance parameters such as rotor speed, compressor pressure ratio and special fuel consumption. The main dynamic equations of a gas turbine system can be derived from the laws of conservation principles. To this aim, the conservation balances for the turbine's overall mechanical energy, internal energy and the gas mass are constructed. In order to achieve an intensive dynamic model which is suitable for process control purposes, one needs to apply the following general assumptions [36]:

- The physical and chemical properties of all parts of the gas turbine, i.e., special heat at constant pressure and constant size, special gas constant and adiabatic index, are fixed.
- Heat loss (heat transfer, heat conduction, radiant heat) is ignored.

Accordingly, the dynamical model of a gas turbine can be presented as [7]:

$$\begin{aligned}
\frac{dm_c}{dt} &= v_c + v_f - v_T \\
\frac{dp_3^{tot}}{dt} &= \frac{R}{V_c c_v}\left(v_c c_p T_1^{tot}\left(1+\eta_C^{-1}\left(\left(\frac{p_3^{tot}}{p_1^{tot}\sigma_c}\right)^{\bar{\kappa}}-1\right)\right)\right. \\
&\quad \left. + Q_f \eta_c v_f - v_T c_p \frac{p_3^{tot} V_c}{m_c R}\right) \\
\frac{dn}{dt} &= \frac{1}{4\pi^2 \Theta n}\left(\frac{v_T c_p V_c \eta_T \eta_m p_3^{tot}}{m_c R}\left(1-\left(\frac{p_1^{tot}}{p_3^{tot}\sigma_I \sigma_N}\right)^{\bar{\kappa}}\right)\right. \\
&\quad \left. - v_C c_p\left(\left(\frac{p_3^{tot}}{p_1^{tot}\sigma_c}\right)^{\bar{\kappa}}-1\right)\frac{T_1^{tot}}{\eta_c} - \frac{3\pi n M_L}{25}\right) \qquad (1)
\end{aligned}$$

where $\bar{\kappa} = \frac{(\kappa-1)}{\kappa}$, $A_3 = c_1 \frac{P_0 T_{03}^{tot}}{P_{03}^{tot}\sigma_N} v_a$, and

$$\begin{aligned}
v_c &= \frac{\beta A_1 p_1^{tot}}{\sqrt{T_1^{tot}}}\left(a_1 n \frac{p_3^{tot}}{p_1^{tot}\sigma_c}\left(\frac{T_1^{tot}}{288.15}\right)^{-0.5}\right. \\
&\quad \left. + a_2 n\left(\frac{T_1^{tot}}{288.15}\right)^{-0.5} + a_3 \frac{p_3^{tot}}{p_1^{tot}\sigma_c} + a_4\right) \qquad (2) \\
v_T &= \frac{\beta A_3 p_3^{tot}}{\sqrt{\frac{p_3^{tot} V_c}{m_c R}}}\left(b_1\left(\frac{p_3^{tot} V_c}{m_c R}\right)^{-0.5} \frac{\tau n p_3^{tot}\sigma_I \sigma_N}{p_1^{tot}}\right. \\
&\quad \left. + b_2\left(\frac{p_3^{tot} V_c}{m_c R}\right)^{-0.5} \tau n + b_3 \frac{p_3^{tot}\sigma_I \sigma_N}{p_1^{tot}} + b_4\right) \qquad (3)
\end{aligned}$$

The total outlet temperature of the turbine is described using the turbine efficiency as

$$T_4^{tot} = \frac{p_3^{tot} V_c}{m_c R}\left(1-\eta_T\left(1-\left(\frac{p_1^{tot}}{p_3^{tot}\sigma_I \sigma_N}\right)^{\bar{\kappa}}\right)\right) \qquad (4)$$

Note that the notation list of the parameters are given in Table 1. The values of the constants and parameters in the given model are known or determined based on the experimental measurements. The details of the parameters estimation and model identification procedure are given in [11]. By defining $u = [u_1 \;\; u_2]^T = [v_f \;\; v_a]^T$ as the control input vector comprising of mass flow rate of fuel (v_f), and power turbine nozzle angle (v_a), $y = [y_1 \; y_2]^T = [n \;\; T_4^{tot}]^T$ as the controlled output vector comprising of rotational speed (n), and outlet total temperature (T_4^{tot}), and assuming p_1^{tot}, T_1^{tot} and M_L as the disturbance signals, then linearizing the equations around the desired operating point of the turbine, one gets the following model

$$\begin{bmatrix} y_1(s) \\ y_2(s) \end{bmatrix} = \begin{bmatrix} G_{11}(s) & G_{12}(s) \\ G_{21}(s) & G_{22}(s) \end{bmatrix}\begin{bmatrix} u_1(s) \\ u_2(s) \end{bmatrix} + \begin{bmatrix} D_1(s) \\ D_2(s) \end{bmatrix} \qquad (5)$$

where $D_1(s)$ and $D_2(s)$ represent the effects of disturbances and uncertainties owing to environmental changes, loading, and internally generated vibration and shock.

III. MODEL PREDICTIVE CONTROL OF GAS TURBINE

For a gas turbine, operating under the specified conditions $m_c = 730.71$, $p_3^{tot} = 208270$ and $n = 0.0043$, a linearized small signal model is obtained by incorporating the results in the previous section and the experimental validations as follows [12]:

$$\begin{bmatrix} T_4 \\ n \end{bmatrix} = \begin{bmatrix} \frac{10^6\,(1.3s+335.998)}{s^2+392s+13900} & \frac{-5.6s^2-246s-744.01}{s^2+28.9s+24.6} \\ \frac{10^6\,(9.04s+283.965)}{s^3+275.7s^2+18510s+365600} & \frac{83.4\,s+6300}{s^2+115s+195} \end{bmatrix} \times \begin{bmatrix} v_f \\ v_a \end{bmatrix} \qquad (6)$$

Choosing a sampling time of 10 ms, the corresponding discrete-time transfer function model is obtained as:

$$\begin{bmatrix} T_4 \\ n \end{bmatrix} = \underbrace{\begin{bmatrix} M_{11}(z^{-1}) & M_{12}(z^{-1}) \\ M_{21}(z^{-1}) & M_{22}(z^{-1}) \end{bmatrix}}_{M(z^{-1})}\begin{bmatrix} v_f \\ v_a \end{bmatrix}$$

$$\begin{aligned}
M_{11}(z^{-1}) &= \frac{8590z^{-1} - 946.3z^{-2}}{1-0.7036z^{-1}+0.01984z^{-2}}, \\
M_{12}(z^{-1}) &= \frac{-5.6+9.024z^{-1}-3.489z^{-2}}{1-1.746z^{-1}+0.7486z^{-2}}, \\
M_{21}(z^{-1}) &= \frac{215z^{-1}-61.13z^{-2}-70.06z^{-3}}{1-1.439z^{-1}+0.6108z^{-2}-0.06346z^{-3}}, \\
M_{22}(z^{-1}) &= \frac{0.716z^{-1}-0.3422z^{-2}}{1-1.305z^{-1}+0.3166z^{-2}} \qquad (7)
\end{aligned}$$

A. CONSTRUCTION OF A CARIMA MODEL FOR GAS TURBINE

Before proceeding to the design of MPC for the gas turbine system, we need to construct an appropriate model incorporating the effects of noises and disturbances affecting the practical system. To this aim, we will consider the following form known as the controlled autoregressive integrated

TABLE 1. The Units and Values of the Parameters in Gas Turbine System.

Notation	Parameter definition	Unit	Value	Notation	Parameter definition	Unit	Value
R	specific gas constant	$\frac{J}{kgK}$	287	β	Specific parameter of air	$\frac{\sqrt{K}s}{m}$	0.0404
c_p	specific heat pressure	$\frac{J}{kgK}$	1004.5	c_v	specific heat volume	$\frac{J}{kgK}$	717.5
κ	adiabatic exponent	-	1.4	τ	turbine velocity coefficient	$\sqrt{K}s$	0.0281
Q_f	lower thermal value of fuel	$\frac{MJ}{kg}$	42.8	A_1	compressor inlet area	m^2	5.87e-3
A_3	turbine inlet area	m^2	11.706e-3	σ_N	Deflector pressure loss coefficient	-	0.9669
σ_I	Inlet duct pressure loss coefficient	-	0.9888	σ_c	Combustion chamber pressure loss coefficient	-	0.9374
η_C	Compressor efficiency	-	0.6759	η_T	Turbine efficiency	-	0.857
η_c	Combustion efficiency	-	0.7916	η_m	Mechanical efficiency	-	0.98
Θ	inertial moment	kgm^2	4e-4	V_c	Combustion chamber volume	m^3	5.675e-3
a_1	Constant coefficient	s	3.53e-4	a_2	Constant coefficient	s	11.097e-4
a_3	Constant coefficient	-	-0.461	a_4	Constant coefficient	-	0.1664
b_1	Constant coefficient	m^2	-3.37e-2	b_2	Constant coefficient	-	44.58e-4
b_3	Constant coefficient	-	0.0488	b_4	Constant coefficient	-	0.1554

moving average (CARIMA) model:

$$A(z^{-1})y(t) = B(z^{-1})u(t) + \frac{\xi(t)}{1-z^{-1}} \tag{8}$$

where $d(t) = \left(1-z^{-1}\right)^{-1}\xi(t)$ denotes the effects of external disturbances, $\xi(t)$ is the white noise with zero mean and variance σ^2. Defining $\Delta = 1 - z^{-1}$, Eq. (8) yields

$$\tilde{A}(z^{-1})y(t) = B(z^{-1})\Delta u(t) + \xi(t) \tag{9}$$

where $\tilde{A}(z^{-1}) = \Delta A(z^{-1})$. It is important to note that both coefficient matrices $\tilde{A}$ and $\tilde{B}$ are polynomial matrices and expressed as

$$\tilde{A}(z^{-1}) = I + \tilde{A}_1 z^{-1} + \ldots + \tilde{A}_{n_a+1} z^{-(n_a+1)} \tag{10}$$

$$B(z^{-1}) = B_1 z^{-1} + \ldots + B_{n_b} z^{-n_b} \tag{11}$$

To obtain such polynomial coefficient matrices of the CARIMA model for the gas turbine system, we first define

$$\tilde{A}(z^{-1}) = \begin{bmatrix} \tilde{A}_{11}(z^{-1}) & 0 \\ 0 & \tilde{A}_{22}(z^{-1}) \end{bmatrix} \tag{12}$$

where $\tilde{A}_{ii}(z^{-1})$, $\forall i = 1, 2$, are defined as the Least Common Multiplier (LCM) of the denominators of $M_{i1}(z^{-1})$ and $M_{i2}(z^{-1})$:

$$\begin{aligned}\tilde{A}_{11} &= 1 - 2.45z^{-1} + 1.997z^{-2} - 0.5614z^{-3} \\ &\quad + 0.01485z^{-4}\end{aligned} \tag{13}$$

$$\begin{aligned}\tilde{A}_{22} &= 1 - 2.744z^{-1} + 2.806z^{-2} - 1.316z^{-3} \\ &\quad + 0.2762z^{-4} - 0.0201z^{-5}\end{aligned} \tag{14}$$

Then, considering the transfer function and CARIMA models, the coefficient matrix $B(z^{-1})$ is simply calculated as

$$\begin{aligned}B(z^{-1}) &= \tilde{A}^{-1}(z^{-1})M(z^{-1}) \\ &= \begin{bmatrix} B_{11}(z^{-1}) & B_{12}(z^{-1}) \\ B_{21}(z^{-1}) & B_{22}(z^{-1}) \end{bmatrix}\end{aligned} \tag{15}$$

where

$$\begin{aligned}B_{11}(z^{-1}) &= 8590z^{-1} - 1.595 \times 10^4 z^{-2} \\ &\quad + 8083z^{-3} - 708.4z^{-4}\end{aligned} \tag{16}$$

$$\begin{aligned}B_{12}(z^{-1}) &= -5.6 + 12.96z^{-1} - 9.95z^{-2} \\ &\quad + 2.634z^{-3} - 0.06922z^{-4}\end{aligned} \tag{17}$$

$$\begin{aligned}B_{21}(z^{-1}) &= 215z^{-1} - 34.7z^{-2} + 77.8z^{-3} \\ &\quad + 72.08z^{-4} - 22.19z^{-5}\end{aligned} \tag{18}$$

$$\begin{aligned}B_{22}(z^{-1}) &= 0.716z^{-1} - 1.373z^{-2} + 0.9299z^{-3} \\ &\quad - 0.2545z^{-4} + 0.02172z^{-5}\end{aligned} \tag{19}$$

B. GAS TURBINE OUTPUT PREDICTION MODEL

The gas turbine CARIMA model is employed to estimate the future behavior of the gas system. Assuming the prediction horizon N_p, and expanding (9), (10) and (11) for $t+1, \cdots, t+N_p$, one obtains

$$\begin{aligned}
&t+1: \\
&\quad y_{t+1} + \tilde{A}_1 y_t + \ldots + \tilde{A}_{n_a+1} y_{t-n_a} \\
&\quad = b_1 \Delta u_t + b_2 \Delta u_{t-1} + \ldots + b_{n_b} \Delta u_{t-n_b+1} \\
&t+2: \\
&\quad y_{t+2} + \tilde{A}_1 y_{t+1} + \ldots + \tilde{A}_{n_a+1} y_{t-n_a+1} \\
&\quad = b_1 \Delta u_{t+1} + b_2 \Delta u_t + \ldots + b_{n_b} \Delta u_{t-n_b+2} \\
&\quad\quad \vdots \qquad\qquad \vdots \\
&t+N_p: \\
&\quad y_{t+N_p} + \tilde{A}_1 y_{t+N_p-1} + \ldots + \tilde{A}_{n_a+1} y_{t-n_a+N_p-1} \\
&\quad = b_1 \Delta u_{t+N_p-1} + b_2 \Delta u_{t+N_p-2} + \ldots + b_{n_b} \Delta u_{t-n_b+N_p}
\end{aligned} \tag{20}$$

We define the following Toeplitz ($\mathcal{T}$) and Hankel ($\mathcal{H}$) matrices:

$$\mathcal{T}_{\tilde{A}} = \begin{bmatrix} I & 0 & \cdots & 0 \\ \tilde{A}_1 & I & \cdots & 0 \\ \tilde{A}_2 & \tilde{A}_1 & \cdots & 0 \\ \vdots & \vdots & \vdots & \vdots \end{bmatrix}, \mathcal{T}_B = \begin{bmatrix} B_1 & 0 & \cdots & 0 \\ B_2 & B_1 & \cdots & 0 \\ B_3 & B_2 & \cdots & 0 \\ \vdots & \vdots & \vdots & \vdots \end{bmatrix} \tag{21}$$

$$\mathcal{H}_{\tilde{A}} = \begin{bmatrix} \tilde{A}_1 & \tilde{A}_2 & \cdots & \tilde{A}_{n_a+1} \\ \tilde{A}_2 & \tilde{A}_3 & \cdots & 0 \\ \tilde{A}_3 & \tilde{A}_4 & \cdots & 0 \\ \vdots & \vdots & \vdots & \vdots \end{bmatrix}$$

$$\mathcal{H}_B = \begin{bmatrix} B_2 & B_3 & \cdots & B_{n_b} \\ B_3 & B_4 & \cdots & 0 \\ B_4 & B_5 & \cdots & 0 \\ \vdots & \vdots & \vdots & \vdots \end{bmatrix} \tag{22}$$

Then, the set of equations in (20) can be expressed in the matrix form as

$$
\begin{aligned}
&\mathcal{T}_{\tilde{A}} \underbrace{\begin{bmatrix} y_{t+1} \\ y_{t+2} \\ \vdots \\ y_{t+N_p} \end{bmatrix}}_{\triangleq \underrightarrow{y}_{t+1}^{t+N_p}} + \mathcal{H}_{\tilde{A}} \underbrace{\begin{bmatrix} y_{t} \\ y_{t-1} \\ \vdots \\ y_{t-n_a} \end{bmatrix}}_{\triangleq \underleftarrow{y}_{t}^{t-n_a}} \\
&= \mathcal{T}_B \underbrace{\begin{bmatrix} \Delta u_{t} \\ \Delta u_{t+1} \\ \vdots \\ \Delta u_{t+N_p-1} \end{bmatrix}}_{\triangleq \underrightarrow{\Delta u}_{t}^{t+N_p-1}} + \mathcal{H}_B \underbrace{\begin{bmatrix} \Delta u_{t-1} \\ \Delta u_{t-2} \\ \vdots \\ \Delta u_{t-n_b+1} \end{bmatrix}}_{\triangleq \underleftarrow{\Delta u}_{t-1}^{t-n_b+1}}
\end{aligned} \tag{23}
$$

Finally, the output prediction vector is obtained as

$$
\begin{aligned}
&\underrightarrow{y}_{t+1}^{t+N_p} \\
&= \underbrace{\mathcal{T}_{\tilde{A}}^{-1}\mathcal{T}_B}_{=H} \underrightarrow{\Delta u}_{t}^{t+N_p-1} + \underbrace{\mathcal{T}_{\tilde{A}}^{-1}\mathcal{H}_B}_{=P} \underleftarrow{\Delta u}_{t-1}^{t-n_b+1} \underbrace{-\mathcal{T}_{\tilde{A}}^{-1}\mathcal{H}_{\tilde{A}}}_{=Q} \underleftarrow{y}_{t}^{t-n_a}
\end{aligned} \tag{24}
$$

In the general case of choosing control horizon less than or equal to the prediction horizon $N_c \leq N_p$, the predictions model is obtained as follows:

$$
\underrightarrow{y}_{t+1}^{t+N_p} = H \underrightarrow{\Delta u}_{t}^{t+N_c-1} + P \underleftarrow{\Delta u}_{t-1}^{t-n_b+1} + Q \underleftarrow{y}_{t}^{t-n_a} \tag{25}
$$

where H_1 denotes the first $N_c n_u$ column of the matrix $H = \mathcal{T}_{\tilde{A}}^{-1}\mathcal{T}_B$.

C. HANDLING DISTURBANCES AND MEASUREMENT NOISES

In the absence of uncertainty/disturbances, offset-free control can be easily obtain without integral action; but in practice, the existence of parameter uncertainties and disturbances necessitate the use of an integrator. Accordingly, the constructed prediction model based on the input increment (Δu) rather than the input (u), introduces an internal integral action in the MPC formulation and leads to an unbiased prediction [37]. This formulation is able to appropriately reject constant disturbances which will be investigated in the followings. On the other hand, measurement noises generally will not degrade using this model because of their high-frequency nature. Considering the prediction model (25), it can be seen that the output prediction will severely affected when the past measured signals, i.e. $\underleftarrow{y}_{t}^{t-n_a}$ and $\underleftarrow{\Delta u}_{t-1}^{t-n_b+1}$, are contaminated with measurement noises. The idea is to use an appropriate low-pass filter to obtain the output prediction model in terms of filtered past signal values. Considering the same filter for both input and output signals, we define the filtered signals $\tilde{y}(t)$ and $\Delta\tilde{u}(t)$ as

$$
\tilde{y}(t) = T^{-1}(z^{-1})y(t) \tag{26}
$$

$$
\Delta\tilde{u}(t) = T^{-1}(z^{-1})\Delta u(t) \tag{27}
$$

where $T^{-1}(z^{-1})$ denotes the filter's transfer function and

$$
T(z^{-1}) = T_0 + T_1 z^{-1} + \cdots + T_{n_f} z^{-n_f} \tag{28}
$$

Using the filtered CARIMA model and following the same procedure in this section, one obtains

$$
\underrightarrow{\tilde{y}}_{t+1}^{t+N_p} = H \underrightarrow{\Delta\tilde{u}}_{t}^{t+N_p-1} + P \underleftarrow{\Delta\tilde{u}}_{t-1}^{t-n_b+1} + Q \underleftarrow{\tilde{y}}_{t}^{t-n_a} \tag{29}
$$

This result expresses the filtered output prediction $\underrightarrow{\tilde{y}}_{t+1}^{t+N_p}$ which cannot be used in the MPC formulation. Rather, one needs to obtain $\underrightarrow{y}_{t+1}^{t+N_p}$ in terms of $\underrightarrow{\Delta u}_{t}^{t+N_p-1}$ and filtered past signal values $\underleftarrow{\Delta\tilde{u}}_{t-1}^{t-n_b+1}$ and $\underleftarrow{\tilde{y}}_{t}^{t-n_a}$. To this aim, using (26) and (27), one obtains $T(z^{-1})\tilde{y}(t) = y(t)$ and $T(z^{-1})\Delta\tilde{u}(t) = \Delta u(t)$. Then, using the same procedure applied to the CARIMA model $\tilde{A}(z^{-1})y(t) = B(z^{-1})\Delta u(t)$ and by comparison, one obtains

$$
\begin{aligned}
&\underrightarrow{\tilde{y}}_{t+1}^{t+N_p} \\
&= \mathcal{T}_{T_y}^{-1}(N_p) \underrightarrow{y}_{t+1}^{t+N_p} - \mathcal{T}_{T_y}^{-1}(N_p)\mathcal{H}_{T_y}(N_p, n_f) \underleftarrow{\tilde{y}}_{t}^{t-n_f+1}
\end{aligned} \tag{30}
$$

$$
\begin{aligned}
&\underrightarrow{\Delta\tilde{u}}_{t}^{t+N_p-1} \\
&= \mathcal{T}_{T_y}^{-1}(N_p) \underrightarrow{\Delta u}_{t}^{t+N_p-1} - \mathcal{T}_{T_y}^{-1}(N_p)\mathcal{H}_{T_y}(N_p, n_f) \underleftarrow{\Delta\tilde{u}}_{t-1}^{t-n_f}
\end{aligned} \tag{31}
$$

Then, combining (29), (30) and (31) results

$$
\begin{aligned}
&\underrightarrow{y}_{t+1}^{t+N_p} \\
&= \mathcal{T}_{T_y}(N_p) H \mathcal{T}_{T_y}^{-1}(N_p) \underrightarrow{\Delta u}_{t}^{t+N_p-1} + \mathcal{T}_{T_y}(N_p) P \underleftarrow{\Delta\tilde{u}}_{t-1}^{t-n_b+1} \\
&\quad - \mathcal{T}_{T_y}(N_p) H \mathcal{T}_{T_y}^{-1}(N_p)\mathcal{H}_{T_y}(N_p, n_f) \underleftarrow{\Delta\tilde{u}}_{t-1}^{t-n_f} \\
&\quad + \mathcal{T}_{T_y}(N_p) Q \underleftarrow{\tilde{y}}_{t}^{t-n_a} + \mathcal{H}_{T_y}(N_p, n_f) \underleftarrow{\tilde{y}}_{t}^{t-n_f+1}
\end{aligned} \tag{32}
$$

Now defining $\bar{n}_b = \max(n_b, n_f+1)$ and $\bar{n}_a = \max(n_a, n_f-1)$, it is easy to verify that

$$
\begin{aligned}
\underleftarrow{\Delta\tilde{u}}_{t-1}^{t-n_b+1} &= \underbrace{\begin{bmatrix} I_{n_u(n_b-1)} & 0_{n_u(n_b-1)\times n_u(\bar{n}_b-n_b)} \end{bmatrix}}_{L_{u1}} \underleftarrow{\Delta\tilde{u}}_{t-1}^{t-\bar{n}_b+1} \\
\underleftarrow{\Delta\tilde{u}}_{t-1}^{t-n_f} &= \underbrace{\begin{bmatrix} I_{n_u n_f} & 0_{n_u n_f\times n_u(\bar{n}_b-n_f-1)} \end{bmatrix}}_{L_{u2}} \underleftarrow{\Delta\tilde{u}}_{t-1}^{t-\bar{n}_b+1} \\
\underleftarrow{\tilde{y}}_{t}^{t-n_a} &= \underbrace{\begin{bmatrix} I_{n_y(n_a+1)} & 0_{n_y(n_a+1)\times n_y(\bar{n}_a-n_a)} \end{bmatrix}}_{L_{y1}} \underleftarrow{\tilde{y}}_{t}^{t-\bar{n}_a} \\
\underleftarrow{\tilde{y}}_{t}^{t-n_f+1} &= \underbrace{\begin{bmatrix} I_{n_y n_f} & 0_{n_y n_f\times n_y(\bar{n}_a-n_f+1)} \end{bmatrix}}_{L_{y2}} \underleftarrow{\tilde{y}}_{t}^{t-\bar{n}_a}
\end{aligned} \tag{33}
$$

Using the above notations, the filtered output prediction model in the general case of $N_c \leqslant N_p$ is obtained as

$$
\begin{aligned}
&\underrightarrow{y}_{t+1}^{t+N_p} = H_{f1} \underrightarrow{\Delta u}_{t}^{t+N_c-1} + P_f \underleftarrow{\Delta\tilde{u}}_{t-1}^{t-\bar{n}_b+1} + Q_f \underleftarrow{\tilde{y}}_{t}^{t-\bar{n}_a}, \\
&\begin{cases} H_f = \mathcal{T}_{T_y}(N_p) H \mathcal{T}_{T_y}^{-1}(N_p) \\ P_f = \mathcal{T}_{T_y}(N_p) P L_{u1} - H \mathcal{H}_{T_y}(N_p, n_f) L_{u2} \\ Q_f = \mathcal{T}_{T_y}(N_p) Q L_{y1} + \mathcal{H}_{T_y}(N_p, n_f) L_{y2} \end{cases}
\end{aligned} \tag{34}
$$

where H_{f1} denotes the first $N_c n_u$ column of the matrix $H_f = \mathcal{T}_{T_y}(N_p)H\mathcal{T}_{T_y}^{-1}(N_p)$.

D. COST FUNCTION AND DESIGN CONSTRAINTS

Different MPC algorithms offer various cost functions to obtain the control law. The main purpose is that the future output on the considered horizon follows the designated reference signal. To design the control law, a specific cost function should be considered that represents the tracking error and the control effort simultaneously. Let define

$$J = \left(\underset{\rightarrow}{r}_{t+1}^{t+N_p} - \underset{\rightarrow}{y}_{t+1}^{t+N_p}\right)^T W_Y \left(\underset{\rightarrow}{r}_{t+1}^{t+N_p} - \underset{\rightarrow}{y}_{t+1}^{t+N_p}\right) + \left(\Delta\underset{\rightarrow}{u}_t^{t+N_c-1}\right)^T W_U \left(\Delta\underset{\rightarrow}{u}_t^{t+N_c-1}\right) \quad (35)$$

where $\underset{\rightarrow}{r}_{t+1}^{t+N_p}$ represents the vector of reference signals over the prediction horizon, and W_Y and W_U are the outputs and inputs weighting matrices, respectively. The weighting matrices are defined as

$$W_U = \begin{bmatrix} W_u & 0 & 0 \\ 0 & \ddots & 0 \\ 0 & 0 & W_u \end{bmatrix}_{N_c n_u \times N_c n_u} \quad (36)$$

$$W_Y = \begin{bmatrix} W_y & 0 & 0 \\ 0 & \ddots & 0 \\ 0 & 0 & W_y \end{bmatrix}_{N_p n_y \times N_p n_y} \quad (37)$$

Substituting (25) into (32), the cost function is rewritten as

$$J = \frac{1}{2}\left(\Delta\underset{\rightarrow}{u}_t^{t+N_c-1}\right)^T S \left(\Delta\underset{\rightarrow}{u}_t^{t+N_c-1}\right) + f^T \Delta\underset{\rightarrow}{u}_t^{t+N_c-1} + J_0 \quad (38)$$

where

$$S = 2\left(H_1^T W_Y H_1 + W_U\right) \quad (39)$$

$$f = 2H_1^T W_Y \left(P\Delta\underset{\leftarrow}{u}_{t-1}^{t-n_b+1} + Q\underset{\leftarrow}{y}_t^{t-n_a} - \underset{\rightarrow}{r}_{t+1}^{t+N_p}\right) \quad (40)$$

$$J_0 = X^T W_Y X$$
$$X = \left(\underset{\rightarrow}{r}_{t+1}^{t+N_p} - P\Delta\underset{\leftarrow}{u}_{t-1}^{t-n_b+1} - Q\underset{\leftarrow}{y}_t^{t-n_a}\right) \quad (41)$$

In the next step, the constraints on the control signal variations and magnitude, and bounds on the output signals are considered:

$$\begin{cases} \underline{\Delta u} \leqslant \Delta u_t \leqslant \overline{\Delta u} & \forall t, t+1, \ldots, t+N_c-1 \\ \underline{u} \leqslant u_t \leqslant \bar{u} & \forall t, t+1, \ldots, t+N_c-1 \\ \underline{y} \leqslant y_t \leqslant \bar{y} & \forall t, t+1, \ldots, t+N_p-1 \end{cases} \quad (42)$$

The constraints of the control signal variations are calculated as

$$\begin{bmatrix} I_{N_c n_u} \\ -I_{N_c n_u} \end{bmatrix} \begin{bmatrix} \Delta u_t \\ \Delta u_{t+1} \\ \vdots 5\Delta u_{t+N_c-1} \end{bmatrix} \leqslant \begin{bmatrix} \overline{\Delta u} \\ \vdots \\ \overline{\Delta u} \\ -\underline{\Delta u} \\ \vdots \\ -\underline{\Delta u} \end{bmatrix}$$
$$\Rightarrow C_{\Delta u}\Delta\underset{\rightarrow}{u}_t^{t+N_c-1} \leqslant d_{\Delta u} \quad (43)$$

and the constraints of the magnitude of control signal are considered as

$$\begin{bmatrix} I_{N_c n_u} \\ -I_{N_c n_u} \end{bmatrix} \begin{bmatrix} u_t \\ u_{t+1} \\ \vdots \\ u_{t+N_c-1} \end{bmatrix} \leqslant \begin{bmatrix} \bar{u} \\ \vdots \\ \bar{u} \\ -\underline{u} \\ \vdots \\ -\underline{u} \end{bmatrix}$$
$$\Rightarrow C_u \underset{\rightarrow}{u}_t^{t+N_c-1} \leqslant d_u \quad (44)$$

The above constraints need to be represented in terms of $\Delta\underset{\rightarrow}{u}_t^{t+N_c-1}$. We have

$$\underset{\rightarrow}{u}_t^{t+N_c-1} = E\Delta\underset{\rightarrow}{u}_t^{t+N_c-1} + Lu_{t-1}$$
$$E = \begin{bmatrix} I_{n_u} & 0 & \cdots & 0 \\ I_{n_u} & I_{n_u} & \cdots & 0 \\ \vdots & \vdots & \vdots & \vdots \\ I_{n_u} & I_{n_u} & \cdots & I_{n_u} \end{bmatrix}, L = \begin{bmatrix} I_{n_u} \\ I_{n_u} \\ \vdots \\ I_{n_u} \end{bmatrix} \quad (45)$$

Therefore, the following result is obtained using (44) and (45):

$$C_u \underset{\rightarrow}{u}_t^{t+N_c-1} \leqslant d_u$$
$$\Rightarrow C_u E\Delta\underset{\rightarrow}{u}_t^{t+N_c-1} \leqslant d_u - C_u L u_{t-1} \quad (46)$$

Similarly, for the output constraints, we have

$$\begin{bmatrix} I_{N_p n_y} \\ -I_{N_p n_y} \end{bmatrix} \begin{bmatrix} y_{t+1} \\ y_{t+2} \\ \vdots \\ y_{t+N_p} \end{bmatrix} \leqslant \begin{bmatrix} \bar{y} \\ \bar{y} \\ \vdots \\ \bar{y} \\ -- \\ -\underline{y} \\ -\underline{y} \\ \vdots \\ -\underline{y} \end{bmatrix}$$
$$\Rightarrow C_y \underset{\rightarrow}{y}_{t+1}^{t+N_p} \leqslant d_y \quad (47)$$

Using (25) and (47), we obtain

$$C_y H_1 \Delta\underset{\rightarrow}{u}_t^{t+N_c-1} \leqslant d_y - C_y P\Delta\underset{\leftarrow}{u}_{t-1}^{t-n_b+1} - C_y Q\underset{\leftarrow}{y}_t^{t-n_a} \quad (48)$$

As a result, by combination of the above-mentioned constraints, one attains

$$E_c\Delta\underset{\rightarrow}{u}_t^{t+N_c-1} \leqslant F_c \quad (49)$$

where

$$F_c = \begin{bmatrix} d_{\Delta u} \\ d_u \\ d_y \end{bmatrix} + \begin{bmatrix} 0 \\ -C_u L \\ 0 \end{bmatrix} u_{t-1} + \begin{bmatrix} 0 \\ 0 \\ -C_y P \end{bmatrix} \Delta\underset{\leftarrow}{u}_{t-1}^{t-n_b+1} + \begin{bmatrix} 0 \\ 0 \\ -C_y Q \end{bmatrix} \underset{\leftarrow}{y}_t^{t-n_a}$$
$$E_c = \begin{bmatrix} C_{\Delta u} \\ C_u E \\ C_y H_1 \end{bmatrix} \quad (50)$$

IV. CONTROL LAW CALCULATION

The main purpose is to determine the sequence of optimal control moves which minimizes the cost function (38) subject to the constraints (49) as:

$$(\underrightarrow{\Delta u}_t^{t+N_c-1})^* = \underset{\underrightarrow{\Delta u}_t^{N_c-1}}{\arg\min} \left\{ \begin{array}{c} \frac{1}{2}\left(\underrightarrow{\Delta u}_t^{t+N_c-1}\right)^T S \left(\underrightarrow{\Delta u}_t^{t+N_c-1}\right) \\ +f^T \underrightarrow{\Delta u}_t^{t+N_c-1} \end{array} \right\}$$
$$\text{Subject To}: \quad E_c \underrightarrow{\Delta u}_t^{t+N_c-1} \leqslant F_c \qquad (51)$$

At each sampling time, the optimization problem (51) is solved and the optimal control law is obtained. But only the value of the first control signal is applied to the system and the same procedure is repeated during the next sampling time by incorporating the new measurement data.

Remark 1: The stability of the closed-loop system under the proposed constrained MPC-based approach is directly based on the analysis and results presented in [41]. Considering the results in the mentioned work, one concludes that in practice, a reasonable selection of tuning parameters leads to a well-posed feasible constrained optimization problem which in turn delivers a stable performance for MPC-based algorithm.

V. SIMULATION RESULTS

In this section, the feasibility and performance of the proposed controller are verified via a set of numerical simulations. Throughout the simulations, all initial values of the turbine are set to zero. It is assumed that the turbine's model involves 20% uncertainty which is applied to the poles of the actual system. Also, the bounded disturbances of magnitude $[-20\ 2]^T$ and high frequency measurement noise have also been involved in the simulations. The parameters of the predictive controller are selected as $N_p = 10$, $N_c = 5$, $W_U = diag\left(\frac{1}{6}, \frac{1}{5}\right)$, and $W_Y = diag\left(\frac{1}{9}, \frac{1}{7}\right)$. For practical verification, the effect of actuators saturation is also considered in the simulations by applying actuator constraints $0 \leq v_f \leq 1.1\ [kg/s]$ and $-30 \leq v_a \leq 30\ [deg]$. To investigate the effectiveness of the proposed control method from different points of view, several scenarios of simulations have been performed, i.e. case-A to case-C, where the quadratic programming solver of MATLAB is used to solve the optimization problem (51).

A. NOMINAL OPERATION

In this case, the nominal performance of the proposed method is investigated without constraints disturbances, uncertainties and measurement noise. The reference signals along with the evolution of the gas turbine's outputs are shown in Figs. 2 and 3. These figures demonstrate the perfect tracking goals of the system. However, as shown in Figs. 2 and 3, it is emphasized that the required actuation to keep the turbine in the desired outputs are higher than the available control signals. Therefore the actuators limitations are violated during the simulations.

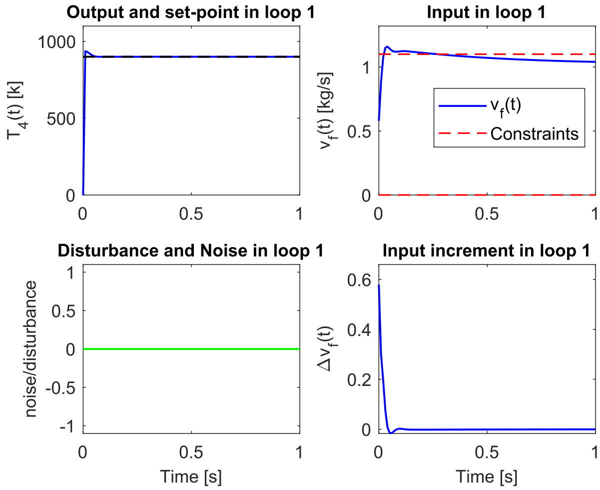

FIGURE 2. Simulation results of loop 1 in case-A (nominal operation).

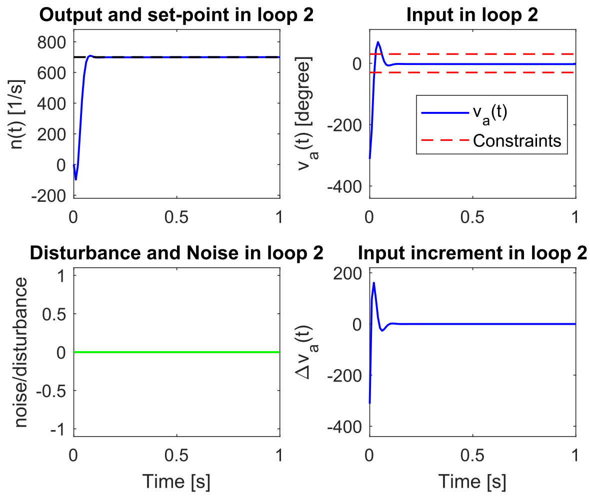

FIGURE 3. Simulation results of loop 2 in case-A (nominal operation).

B. ROBUST PERFORMANCE WITHOUT FILTERING

Here, we aim to investigate the robust performance of the closed-loop system to achieve design objectives in the presence of bounded uncertainties in the turbine's model, unknown disturbances and measurement noise. To this aim, it is assumed that 20% uncertainty is involved in the model and a bounded unknown disturbance with magnitude $[-20\ 2]^T$ is applied to the system during 0.3 to 0.7 second. Note that the disturbance amplitude is quite comparable to the amplitude of the applied control signals and thus, it can deflect the gas turbine from the desired outputs. The simulation results are provided in Figs. 4 and 5. According to the results, one can conclude that the proposed controller is robust against the existing uncertainties/disturbances and can achieve the control objectives while all constraints are guaranteed to be satisfied (no constraints violation). In other words, it is important to note that both actuator signals v_f and v_a satisfy their constraints unlike the nominal case where constraints are not considered. However, as can be seen from simulation results, the measurement noise has sever impact

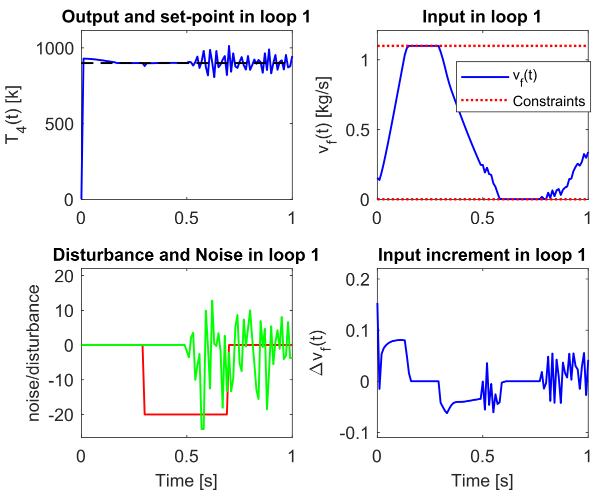

FIGURE 4. Simulation results of loop 1 in case-B (robust performance without filtering).

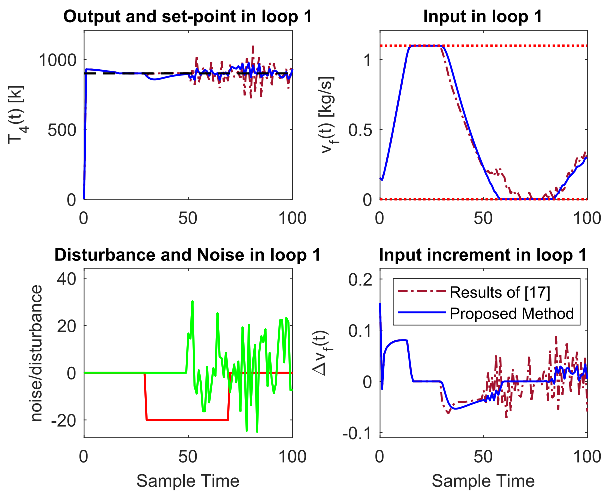

FIGURE 6. Comparison results of loop 1 in case-C (robust performance with measurement noise handling).

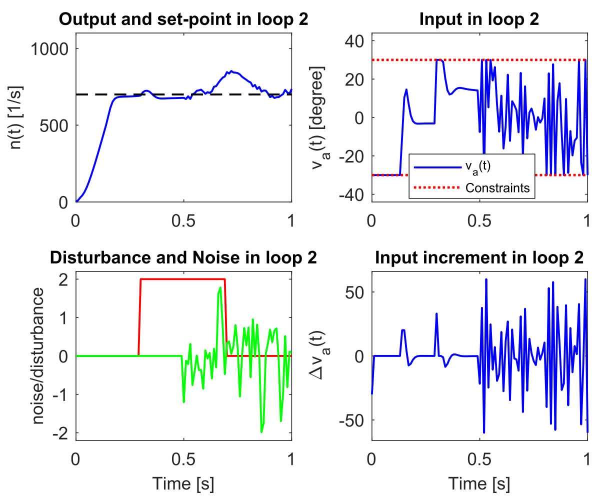

FIGURE 5. Simulation results of loop 2 in case-B (robust performance without filtering).

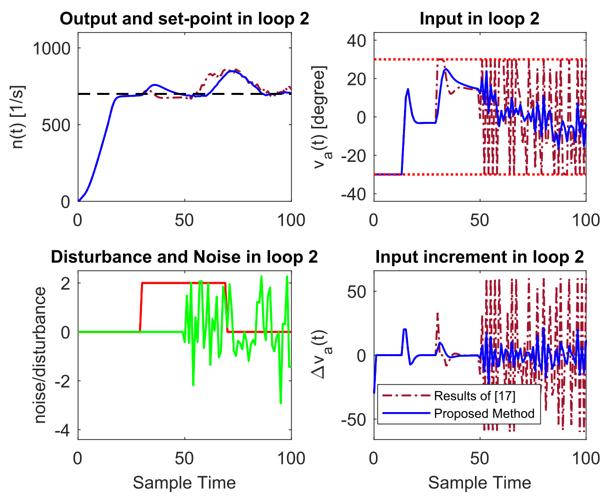

FIGURE 7. Comparison results of loop 2 in case-C (robust performance with measurement noise handling).

not only on the turbine's outputs, but also it leads to high frequency actuation on the actuators which can considerably degrade the performance of the closed-loop system.

C. ROBUST PERFORMANCE WITH MEASUREMENT NOISE HANDLING

Finally, we evaluate the performance of the closed-loop system in the case that the measurements are corrupted by sensors noise. Furthermore, in order to demonstrate the superiority of the proposed method, the proposed approach in [17] is also applied to the gas turbine studied in this article, and the comparison results are illustrated in Figs. 6 and 7. As shown in the figures, the measurement noise can degrade the performance of the closed-loop system to a large extent when the method of Figs. 6 and 7. This performance degradation relies on the fact that there is not any systematic procedure in [17] to cope with the measurement noise. On the contrary, in the current work, as discussed in the previous section (Eqs. (28) and (34)), an efficient systematic procedure is proposed to simultaneously cope with actuator constraints, disturbances and measurement noises. Here, a second-order low-pass filter with $T(z^{-1}) = 1 - 1.6z^{-1} + 0.64z^{-2}$ is used in the structure of the predictive controller. Then, the simulation results are given in Figs. 6 and 7. In this simulation, the same uncertainties/disturbances and actuators limitations as discussed in the previous case are involved. It can be seen that the effects of the measurement noise on the turbine's output have effectively been reduced. Finally, it is worth noting that by taking the advantages of the proposed filtering procedure into account the performance of the closed-loop system is considerably improved without any remarkable effects on the tracking and disturbance rejection performances.

VI. CONCLUSION

According to the studies conducted in this article, the Rouen model is an appropriate choice for controller validation. Therefore, by incorporating proper simulations and competitions, an optimal controller for the gas turbine can be obtained. It is observed that the predictive controller offers very good responses in the gas turbine operating range. The presented responses, not only are in a predetermined suitable range, but also track the reference signal more quickly and without overshoot. It is found that the controller stabilizes the turbine shaft speed outputs and the air temperature of the turbine outlet in the presence of perturbations, noise and uncertainties. Moreover, the constrained predictive controller is able to efficiently remove the outputs undesirable overshoots in the presence of constraints and leads to faster output responses.

REFERENCES

[1] F. Jabari, H. Ghaebi, B. Mohammadi-Ivatloo, M. Mohammadpourfard, and M.-B. Bannae-Sharifian, "Design, worst case study, and sensitivity analysis of a net-zero energy building for sustainable urban development," *Sustain. Cities Soc.*, vol. 54, Mar. 2020, Art. no. 101991.

[2] L. S. Langston, "Aspects of gas turbine thermal efficiency," *Mech. Eng.*, vol. 142, no. 9, pp. 54–55, Sep. 2020.

[3] K. H. M. Al-Hamed and I. Dincer, "A new direct ammonia solid oxide fuel cell and gas turbine based integrated system for electric rail transportation," *eTransportation*, vol. 2, Nov. 2019, Art. no. 100027.

[4] Z. Yu, M. T. Timko, S. C. Herndon, R. C. Miake-Lye, A. J. Beyersdorf, L. D. Ziemba, E. L. Winstead, and B. E. Anderson, "Mode-specific, semi-volatile chemical composition of particulate matter emissions from a commercial gas turbine aircraft engine," *Atmos. Environ.*, vol. 218, Dec. 2019, Art. no. 116974.

[5] A. Imani and M. Montazeri-Gh, "A multi-loop switching controller for aircraft gas turbine engine with stability proof," *Int. J. Control, Autom. Syst.*, vol. 17, no. 6, pp. 1359–1368, Jun. 2019.

[6] J. Seo, H.-S. Lim, J. Park, M. R. Park, and B. S. Choi, "Development and experimental investigation of a 500-W class ultra-micro gas turbine power generator," *Energy*, vol. 124, pp. 9–18, Apr. 2017.

[7] A. Giostri, M. Binotti, C. Sterpos, and G. Lozza, "Small scale solar tower coupled with micro gas turbine," *Renew. Energy*, vol. 147, pp. 570–583, Mar. 2020.

[8] M. Chmielewski, P. Niszczota, and M. Gieras, "Combustion efficiency of fuel-water emulsion in a small gas turbine," *Energy*, vol. 211, Nov. 2020, Art. no. 118961.

[9] D. H. Shin, M. Kim, J. S. Kim, B. J. Lee, and J. Lee, "Precise infrared thermometry with considering background radiation for gas turbine air cooling application," *Int. J. Thermal Sci.*, vol. 158, Dec. 2020, Art. no. 106534.

[10] E. C. Okafor, K. D. K. A. Somarathne, R. Ratthanan, A. Hayakawa, T. Kudo, O. Kurata, N. Iki, T. Tsujimura, H. Furutani, and H. Kobayashi, "Control of NOx and other emissions in micro gas turbine combustors fuelled with mixtures of methane and ammonia," *Combustion Flame*, vol. 211, pp. 406–416, Jan. 2020.

[11] X. Zhou, F. Lu, W. Zhou, and J. Huang, "An improved multivariable generalized predictive control algorithm for direct performance control of gas turbine engine," *Aerosp. Sci. Technol.*, vol. 99, Apr. 2020, Art. no. 105576.

[12] G. Hou, L. Gong, Z. Yang, and J. Zhang, "Multi-objective economic model predictive control for gas turbine system based on quantum simultaneous whale optimization algorithm," *Energy Convers. Manage.*, vol. 207, Mar. 2020, Art. no. 112498.

[13] A. Bonfiglio, S. Cacciacarne, M. Invernizzi, D. Lanzarotto, A. Palmieri, and R. Procopio, "A sliding mode control approach for gas turbine power generators," *IEEE Trans. Energy Convers.*, vol. 34, no. 2, pp. 921–932, Jun. 2019.

[14] M. Schulze, T. Hummel, N. Klarmann, F. Berger, B. Schuermans, and T. Sattelmayer, "Linearized euler equations for the prediction of linear high-frequency stability in gas turbine combustors," *J. Eng. Gas Turbines Power*, vol. 139, no. 3, pp. 031510-1–031510-10, Mar. 2017.

[15] E. P. Petrov, "Stability analysis of multiharmonic nonlinear vibrations for large models of gas turbine engine structures with friction and gaps," *J. Eng. Gas Turbines Power*, vol. 139, no. 2, pp. 022508-1–022508-10, Feb. 2017.

[16] D.-J. Kim, Y.-H. Moon, B.-S. Choi, H.-S. Ryu, and H.-K. Nam, "Impact of a heavy-duty gas turbine operating under temperature control on system stability," *IEEE Trans. Power Syst.*, vol. 33, no. 4, pp. 4543–4552, Jul. 2018.

[17] V. H. Haji, A. Fekih, C. A. Monje, and R. F. Asfestani, "Adaptive model predictive control design for the speed and temperature control of a V94. 2 gas turbine unit in a combined cycle power plant," *Energy*, vol. 207, Sep. 2020, Art. no. 118259.

[18] B. Pongrácz, P. Ailer, K. M. Hangos, and G. Szederkényi, "Nonlinear reference tracking control of a gas turbine with load torque estimation," *Int. J. Adapt. Control Signal Process.*, vol. 22, no. 8, pp. 757–773, Oct. 2008.

[19] P. Ailer, B. Pongracz, and G. Szederkenyi, "Constrained control of a low power industrial gas turbine based on input-output linearization," in *Proc. Int. Conf. Control Autom.*, Jun. 2005, pp. 368–373.

[20] J. Mu and D. Rees, "Approximate model predictive control for gas turbine engines," in *Proc. Amer. Control Conf.*, 2004, pp. 5704–5709.

[21] N. A. Elkhateeb, R. I. Badr, and A. A. Abouelsoud, "Constrained linear state feedback controller for a low-power gas turbine model," *J. Control Eng. Technol.*, vol. 4, no. 1, pp. 66–75, 2014.

[22] R. Whalley and M. Ebrahimi, "Automotive gas turbine regulation," *IEEE Trans. Control Syst. Technol.*, vol. 12, no. 3, pp. 465–473, May 2004.

[23] N. Hajji, S. Maraoui, L. Chrifi-Alaoui, and K. Bouzrara, "Nonlinear distributed model predictive control for complex systems: Application for hydraulic system," *Trans. Inst. Meas. Control*, vol. 41, no. 10, pp. 2751–2763, Jun. 2019.

[24] V. Adetola, D. DeHaan, and M. Guay, "Adaptive model predictive control for constrained nonlinear systems," *Syst. Control Lett.*, vol. 58, no. 5, pp. 320–326, May 2009.

[25] H. Xiao and C. L. P. Chen, "Leader-follower consensus multi-robot formation control using neurodynamic-optimization-based nonlinear model predictive control," *IEEE Access*, vol. 7, pp. 43581–43590, 2019.

[26] T. Jin, X. Shen, T. Su, and R. C. C. Flesch, "Model predictive voltage control based on finite control set with computation time delay compensation for PV systems," *IEEE Trans. Energy Convers.*, vol. 34, no. 1, pp. 330–338, Mar. 2019.

[27] H. Gao, B. Wu, D. Xu, and N. R. Zargari, "A model predictive power factor control scheme with active damping function for current source rectifiers," *IEEE Trans. Power Electron.*, vol. 33, no. 3, pp. 2655–2667, Mar. 2018.

[28] C. Bordons and F. Garcia-Torres, *Model Predictive Control of Microgrids*. Cham, Switzerland: Springer, 2020.

[29] K. Ghanbarpour, F. Bayat, and A. Jalilvand, "Dependable power extraction in wind turbines using model predictive fault tolerant control," *Int. J. Electr. Power Energy Syst.*, vol. 118, Jun. 2020, Art. no. 105802.

[30] H. Bahmani, F. Bayat, and M. Golchin, "Wind turbines power regulation using a low-complexity linear parameter varying-model predictive control approach," *Trans. Inst. Meas. Control*, vol. 42, no. 1, pp. 81–93, Jan. 2020.

[31] T. Manzoor, Z. Sun, Y. Xia, and D. Ma, "MPC based compound flight control strategy for a ducted fan aircraft," *Aerosp. Sci. Technol.*, vol. 107, Dec. 2020, Art. no. 106264.

[32] F. Bayat, "Model predictive sliding control for finite-time three-axis spacecraft attitude tracking," *IEEE Trans. Ind. Electron.*, vol. 66, no. 10, pp. 7986–7996, Oct. 2019.

[33] C. Dai, C. Zong, and G. Chen, "Path tracking control based on model predictive control with adaptive preview characteristics and speed-assisted constraint," *IEEE Access*, vol. 8, pp. 184697–184709, 2020.

[34] M. Ghaedi, F. Bayat, A. Fekih, and S. Mobayen, "Robust performance improvement of lateral motion in four-wheel independent-drive electric vehicles," *IEEE Access*, vol. 8, pp. 203146–203157, 2020.

[35] M. Mohammadkhani, F. Bayat, and A. A. Jalali, "Robust output feedback model predictive control: A stochastic approach," *Asian J. Control*, vol. 19, no. 6, pp. 2085–2096, Nov. 2017.

[36] P. Ailer, I. Santa, and G. Szederkenyi, "Nonlinear model-building of a low-power gas turbine," *Periodica Polytechnica Transp. Eng.*, vol. 29, nos. 1–2, pp. 117–135, 2001.

[37] E. F. Camacho and C. B. Alba, *Model Predictive Control*. London, U.K.: Springer-Verlag, 2007.

[38] G. Hou, L. Gong, C. Huang, and J. Zhang, "Fuzzy modeling and fast model predictive control of gas turbine system," *Energy*, vol. 200, Jun. 2020, Art. no. 117465.

[39] T. S. Pires, M. E. Cruz, M. J. Colaço, and M. A. C. Alves, "Application of nonlinear multivariable model predictive control to transient operation of a gas turbine and NOX emissions reduction," *Energy*, vol. 149, pp. 341–353, Apr. 2018.

[40] A. P. Wiese, M. J. Blom, C. Manzie, M. J. Brear, and A. Kitchener, "Model reduction and MIMO model predictive control of gas turbine systems," *Control Eng. Pract.*, vol. 45, pp. 194–206, Dec. 2015.

[41] D. Mayne, J. Rawlings, C. Rao, and P. Scokaert, "Constrained model predictive control: Stability and optimality," *Automatica*, vol. 36, no. 6, pp. 789–814, 2000.

ALI NASIRI was born in Dezfool, Iran, in 1992. He received the B.S. degree in control engineering from the Jundi-Shapur University of Technology, Dezfool, in 2016, and the M.S. degree in control engineering from the University of Zanjan, Zanjan, Iran, in 2019. His research interests include industrial control theories, gas turbine stability, robust tracking, and model predictive control.

FARHAD BAYAT (Member, IEEE) was born in Zanjan, Iran, in 1981. He received the Ph.D. degree in electrical engineering from the Iran University of Science and Technology, Tehran, Iran, in 2011. Since 2008, he has been with the University of Zanjan, Zanjan, serving as a Lecturer, was appointed as an Assistant Professor in 2011, and then promoted as an Associate Professor in 2016. He was a Visiting Researcher with the Department of Engineering Cybernetics, Norwegian University of Science and Technology, in 2010. He is currently an Associate Professor with the Department of Engineering, University of Zanjan. His research interests include model predictive control, nonlinear robust control, optimization based control, and the aerospace applications of control.

Dr. Bayat is a member of the IEEE community. He has served as a Reviewer for several international journals, including *Automatica*, the IEEE TRANSACTIONS ON INDUSTRIAL ELECTRONICS, the IEEE TRANSACTIONS ON AUTOMATIC CONTROL, IEEE ACCESS, and *Control Engineering Practice*.

SALEH MOBAYEN received the B.Sc. and M.Sc. degrees in control engineering from the University of Tabriz, Tabriz, Iran, in 2007 and 2009, respectively, and the Ph.D. degree in control engineering from Tarbiat Modares University, Tehran, Iran, in January 2013. From February 2013 to December 2018, he was as an Assistant Professor and a Faculty Member with the Department of Electrical Engineering of University of Zanjan, Zanjan, Iran. Since December 2018, he has been an Associate Professor of control engineering with the Department of Electrical Engineering, University of Zanjan. He is currently an Associate Professor with the National Yunlin University of Science and Technology, where he is also with the Future Technology Research Center. His research interests include control theory, sliding mode control, robust tracking, non-holonomic robots, and chaotic systems.

S. HASSAN HOSSEINNIA (Senior Member, IEEE) received the Ph.D. degree *(summa cum laude)* in electrical engineering specializing in automatic control: application in mechatronics from the University of Extremadura, Badajoz, Spain, in 2013. He has an industrial background with ABB, Vasteras, Sweden. Since 2014, he has been an Assistant Professor with the Department of Precision and Microsystems Engineering, TU Delft, Delft, The Netherlands. His current research interests include precision mechatronic system design, precision motion control, and mechatronic system with distributed actuation and sensing.

Dr. Hosseinnia has been an Associate Editor of the *International Journal of Advanced Robotic Systems*, since 2017.